New Investigations on Critical Wall Shear Stresses of CuNi Alloys in Natural and Artificial Seawater

C. Kapsalis[1], G. Schmitt[2], R. Feser[3], B. Sagebiel[1], S. Wilmes[2], M. Macziek[4]

[1] KME Germany AG & Co KG, Klosterstr. 29, D-49074 Osnabrück, Germany
christos.kapsalis@kme.com; bernd.sagebiel@kme.com

[2] IFINKOR-Institute for Maintenance and Corrosion Protection Technology
Kalkofen 4, D-58638 Iserlohn, Germany
guenter.schmitt@ifinkor.de

[3] Laboratory for Corrosion Protection, South-Westfalia University of Applied Sciences
Frauenstuhlweg 31, D-58644 Iserlohn, Germany
feser.r@fh-swf.de

[4] EUCARO BUNTMETAL GmbH, Senator-Helmken-Straße 3, D-28197 Bremen, Germany
Macziek@eucaro.de

ABSTRACT

Recent investigations on critical wall shear stresses for CuNi 90/10 in artificial ASTM seawater revealed that CuNi 90/10 can endure much higher wall shear stresses than generally reported in the literature. These results raised again the question on the validity of corrosion results obtained in ASTM seawater for the prediction of materials performance in natural seawater. The major difference is the formation of biofilms known to play a significant role. The justifications for the previous experiments in ASTM seawater were that the flow velocities applied were above the adherence limits of marine biofilms and that the focus of the work was on the effect of disinfectants, in the presence of which biofilms should not exist. Nevertheless, a comparative study was launched to evaluate the critical wall shear stresses of CuNi 90/10 and CuNi 70/30 in untreated and chlorinated artificial ASTM seawater and natural sea water. The results confirmed that the CuNi alloys perform very similar in both environments and that the flow resistance of these alloys is significantly higher that reported in the literature. The resistance to flow induced localized corrosion (FILC) depends on the alloy composition, the nature of protective corrosion product layers formed during different surface treatment procedures and the presence and concentration of hypochlorite.

Keywords: UNS C70600, CuNi 90/10, UNS C71500, CuNi 70/30, artificial seawater, substitute seawater, natural seawater, wall shear stress, critical wall shear stress, flow, erosion corrosion, flow induced localized corrosion, impinging jet, electrochemical noise

1 INTRODUCTION

It is well documented [1] that FILC is likely to occur only above critical local flow intensities (Fig. 1) creating local energy densities which are high enough to break down protective scales, layers or films on the metal surface. Once removed the high local flow intensities prevent the re-formation of protective layers and, hence, start fast mass transport controlled local metal dissolution (FILC, also called erosion corrosion).

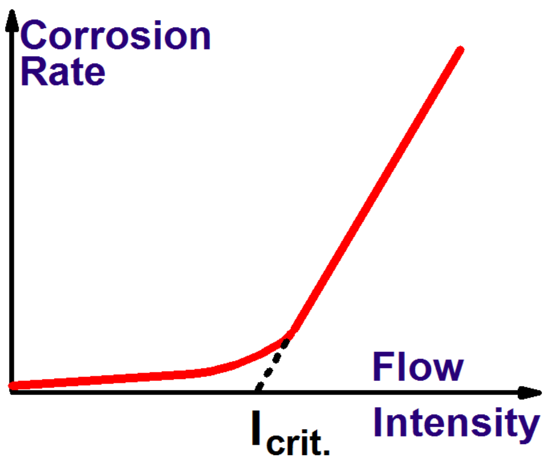

Although often used in technical discussions, the flow velocity measured in [m/s] is not the appropriate physical term to describe the flow intensity because in this term the corrosive flow effect depends on geometric parameters (e.g. pipe diameter). A more general, geometry independent term, is the wall shear stress τ_w measured in [N/m^2] or [Pa] (equ. 1).

$$\tau_w = \mu \left(\frac{du}{dy}\right)_{y=0} \qquad (1)$$

The wall shear stress, defined by equ. 1 (μ = hydrodynamic viscosity [Ns/m^2]; u = flow velocity [m/s]; y = distance from the wall), describes the friction between the fluid and the wall and is therefore the better term to describe the hydrodynamic forces which destroy protective layers and initiate FILC. Calculations and measurements have shown that even the wall shear stress is not directly responsible for the destruction of protective scales, because wall shear stresses encountered in technical flow systems only range in the order of 1 to 100 Pa, in very extreme cases 1 to 100 kPa. However, the adherence forces of scales are found to range in the order of 1 to 10 MPa and the fracture stress of scales in the order of 10 to 100 MPa. This shows that wall shear stresses are several orders of magnitude to weak to destroy protective scales. It was found that forces in high energy microturbulence elements oriented perpendicularly to the wall are finally responsible for the scale destruction (Freak Energy

Density (FED)-Model) [1, 3]. The maximum FED in a flow system can be measured with appropriate tools [2], however, in practical cases this is not necessary, because in a given flow system the FED is proportional to the wall shear stress by a factor in the order of 10^5 to 10^6 [1-4]. Thus, for practical application and flow system evaluations wall shear stresses can be used to quantify flow intensities in given flow systems.

For the selection of materials for technical flow systems it is extremely important to know the critical wall shear stresses τ_{crit}, beyond which FILC is initiated. The critical wall shear stress depends on the type of metal and the properties of the environment, because both metal and environment influence the mechanical and electrochemical properties and, hence, the protectivity of the scales formed under given conditions. It is e.g. known that τ_{crit} can be significantly increased for a given metal in a given flow system by applying the right type and concentration of corrosion inhibitor [5].

Materials selection for flow systems with natural seawater depends on the FILC resistance of the material in this medium. Copper and its alloys are well known for a long time to be highly corrosion resistant in clean natural seawater due to the formation of protective layers and excellent resistance to biofouling [6-8]. Therefore, already some time ago efforts have been made to evaluate the critical wall shear stress for selected copper materials in natural seawater. Some published data are collected in Tab. 1.

TABLE 1 - Critical wall shear stresses of copper base alloys in natural seawater [9, 10]

Material	**Critical Wall Shear Stress [Pa] ([lbf/ft^2])**
Cu	9.6 (0.2)
Al-Brass	19.2 (0.4)
CuNi 90/10	43.1 (0.9)
CuNi 70/30	47.0 (1.0)
CuNi18FeMnCr (80/18/1/1/0.3-0.7)	296,9 (6.2)

Recently new investigations on critical wall shear stresses have been performed on CuNi 90/10 in artificial seawater (ASTM D1141) using the rotated cage method [11] and the electrochemically controlled submersed impinging jet method [12]. According to the results obtained, CuNi 90/10 can endure much higher wall shear stresses than 43 Pa (Table 1), even in the presence of 5 ppm hypochlorite, before FILC was initiated. Data reported ranged in the order of 200 Pa and above [11, 12].

These results prompted again the discussion on the question: How valid are results of corrosion measurements obtained in ASTM seawater for the prediction of the real materials performance in natural seawater? This discussion is not new and has been going on since decades. In most cases the majority of experts believed that results in artificial seawater are different from the materials behaviour in natural seawater. They explained this with the biofilm which is formed on the metal in natural seawater, but not in artificial (substitute) seawater. And the biofilm would change the whole corrosion performance. Therefore, to get reliable results on materials performance in natural seawater the experiments should be executed at the seaside with natural seawater and not inland with substitute seawater.

This status of the discussion was also known to the authors of ref. [11] and [12]. Their justification to launch an experimental program on the flow performance of CuNi alloys in substitute seawater was that the chosen flow intensities were significantly higher than the threshold flow intensities up to which biofilms can adhere to the metal surface and influence its corrosion performance. Furthermore, as the work was focussed on the disinfection with hypochlorite, it was assumed that in fast flowing hypochlorite containing natural sea water no biofilm growth should be expected. Therefore, the biofilm argument should be negligible.

Although convinced that under the conditions chosen no biofilm would occur in any of the seawater types and, therefore, eliminate the main argument against substitute seawater, it was decided to run comparative experiments in natural seawater. The chosen test site was Helgoland, a German island in 40 km distance from the mainland. The experiments were performed in the Biologische Anstalt Helgoland (BAH) which is part of the Stiftung Alfred-Wegener-Institute for Polar and Marine Research, using once-flow-through natural seawater.

2 EXPERIMENTAL

2.1 ECN Controlled Jet Impingement

Under defined flow and geometric conditions the submerged jet (Fig. 2) develops defined wall shear stresses at impinged surfaces which can be calculated according to the empiric equ. 2 developed by Giralt and Trass [13, 14]

$$\tau_w = 0.0447 \cdot \rho \cdot u_0^2 \cdot \mathrm{Re}^{-0.182} (\frac{x}{d})^{-2} \qquad (2)$$

where ρ is the density of the liquid [g/m^3], u_0 is the flow velocity [m/s] at the mouth of the jet nozzle, *Re* the Reynolds number, ν the kinematic viscosity [m^2/s], *d* the inner diameter of the jet nozzle [m] and *x* the radial distance [m] from the impinging centre of the jet on the impinged surface.

In the jet impingement experiments with substitute seawater [ASTM 1141] described in this paper the following data applied: ρ = 1024.91 kg/m^3, ν = 1.025 · 10^{-6} m^2/s, *x* = 0.003 m, *d* = 0,001 m. For the natural Helgoland seawater the following data were used: ρ = 1034.91 kg/m^3, ν = 1.025 · 10^{-6} m^2/s (which is the same as for artificial seawater), pH = 7.9, oxygen concentration 6.8 mg/L, seawater inlet temperature T = 15-19°C. The distance between the mouth of the jet nozzle and the impinged surface was 5 mm. Under these conditions equ. 2 calculates wall shear stresses on the impinged surface in a distance of 3 to 5 mm from the impinging centre of the jet nozzle.

The equation for the calculation of the wall shear stress at a given mass flow rate at the jet nozzle develops the following way:

With equ. 3 for the Reynolds number

$$\mathrm{Re} = \frac{u_0 \cdot d}{\nu} \tag{3}$$

and equ. 4 for the velocity at the mouth of the jet nozzle

$$u_0 = \frac{F_V}{1/4 \cdot \pi \cdot d^2} = \frac{4 F_m}{\pi \cdot \rho \cdot d^2} \tag{4}$$

equ. 5 results for the calculation of the wall shear stress

$$\tau_w = 0{,}00693 \cdot \frac{F_m^{1{,}818} \cdot \nu^{0{,}182}}{\rho^{0{,}818} \cdot d^{1{,}818} \cdot x^2} \tag{5}$$

with F_m: mass flow rate of liquid [kg/s], F_v: volume flow rate of the liquid [m^3/s].

Equ. 5 converts to equ. 6 using ρ = 1024,91 kg/m^3, ν = 1,025·10^{-6} m^2/s, x = 0,003 m and d = 0,001 m for the wall shear stress on the impinged surface in a distance of 3 mm from the centre of the impinging jet nozzle. The only variable is the mass flow rate F_m.

$$\tau_w = 613766\, kg^{-0{,}818} m^{-1} s^{-0{,}182} \cdot F_m^{1{,}818} \tag{6}$$

The impinged surface consisted of two metal electrodes (electrode no. 1 and electrode no.2) positioned centrically under the jet nozzle (Fig. 3). The electrodes were machined from rods of CuNi 90/10 and CuNi 70/30. The chemical composition of the CuNi alloys tested are summarized in Tab. 2. The metal disc (5 mm thick) was cut axially into two halfs. Each half was soldered to a copper wire, and then autophoretically coated and embedded in epoxy resin in a stainless steel electrode holder (Fig. 4, 5). The electrode holder was positioned in a jet cell schematically sketched in Fig. 6. The electrode holder, mounted into the jet cell bottom, is shown in Fig. 7.

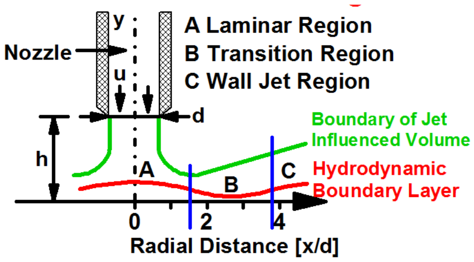

FIGURE 2 - Flow pattern at the submerged impinging jet

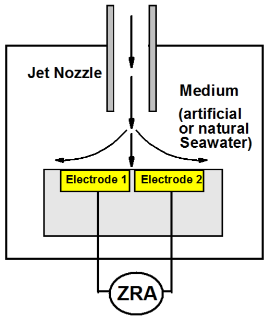

FIGURE 3 - ECR control of FILC initiation during surface impinging

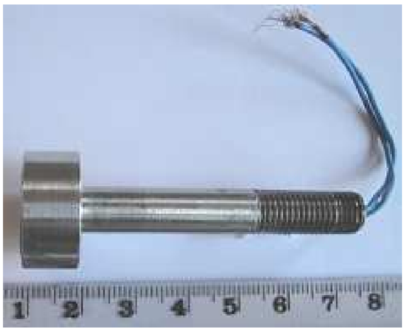

FIGURE 4 - Holder for impinged electrodes

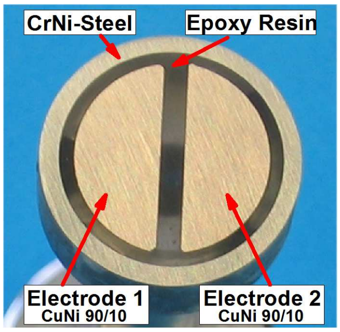

FIGURE 5 - Impinged electrodes embedded in epoxy resin

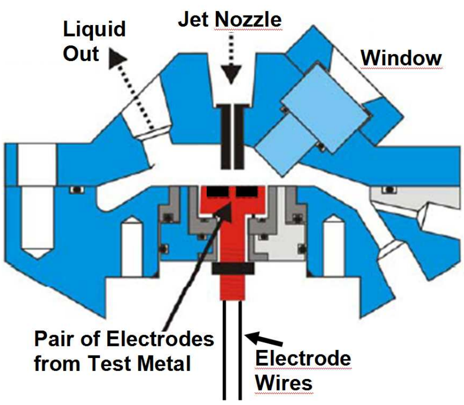

FIGURE 6 - Sketch of jet cell (high pressure) with impinged electrodes

FIGURE 7 - Impinged electrodes positioned in the bottom of the jet cell

TABLE 2 - Chemical composition of the CuNi alloys tested [mass-%]

CuNi Alloy	Ni	Fe	Mn	Sn	C	Pb	P	S	Zn	Co	Cu
CuNi 90/10	10.0-11.0	1.50 - 1.8	0.6 - 1.0	0.03	0.02	0.01	0.02	0.005	0.05	0.1	Rem.
CuNi 70/30	29.0 - 33.0	0.4 - 1.0	1.0	0.03	0.05	0.01	0.02	0.02	0.05	0.1	Rem.

Single values represent the maximum content.

The medium-contacted surface area of each electrode was 0,725 cm^2. During jet impingement the time-related element currents flowing between the two electrodes were measured with a zero resistance ammeter (ZRA) Type IPS/AJ ZRA-FG-A (IPS-Ingenieurbuero Peter Schrems, Germany). For data evaluation the DC part was subtracted from the raw noise data and the values of the noise currents were added in short time intervals (0.05 s) yielding a total noise charge curve with always positive slope. This earlier developed 'Coulombs Counting' method has been reported in Lit. [15, 16]. In case of low uniform corrosion activity on both electrodes, the time-related noise charge curve exhibits a low slope (Fig. 8). When FILC is initiated the noise activity increases and, hence, the slope of the noise charge curve increases. Thus, the change of the noise charge curve indicates in real time the onset of FILC (Fig. 8).

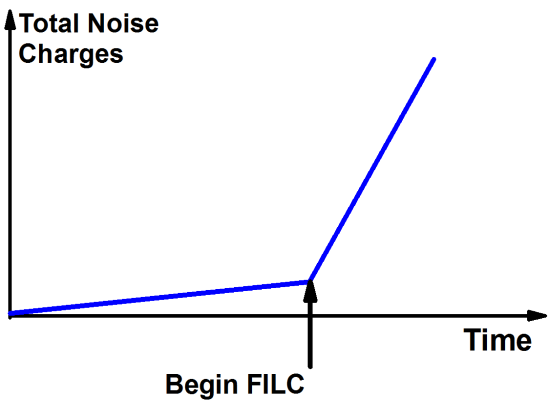

FIGURE 8 - Onset of FILC at increase of total noise charges vs. time curve

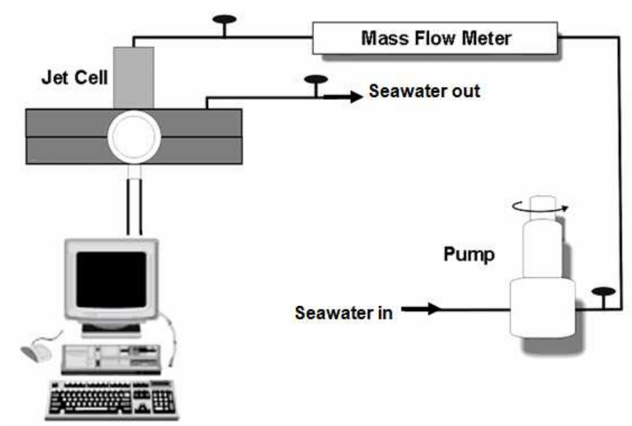

FIGURE 9 - Once-flow-through test rig for jet impingement tests with natural seawater

The experimental setup for jet impingement with natural seawater in a once-flow-through mode is sketched in Fig. 9, a photograph of the test rig installed on the Isle of Helgoland in the Biologische Anstalt is shown in Fig. 10. A 15 ltr. buffer tank was filled with seawater from a seawater tap. From this tank a gear pump with variable transport rate transported the test liquid via a mass flow meter into the jet nozzle (red arrows in Fig. 10). The outflow from the jet cell was drained in case of natural seawater or was re-circulated into the buffer tank in case of experiments with hypochlorite addition. In this case a sodium hypochlorite solution was metered with a dosage pump into the buffer tank which was stirred by an electric stirrer. A separate pump transported the test liquid to a bypass where a chlorine/hypochlorite electrode (model CS2.3, Sensortechnik Meinsberg GmbH, Germany) was positioned (blue arrows in Fig. 10) which measured the hypochlorite concentration and - via a transducer (MU2060, Sensortechnik Meinsberg GmbH) - triggered a sodium hypochlorite dosage pump

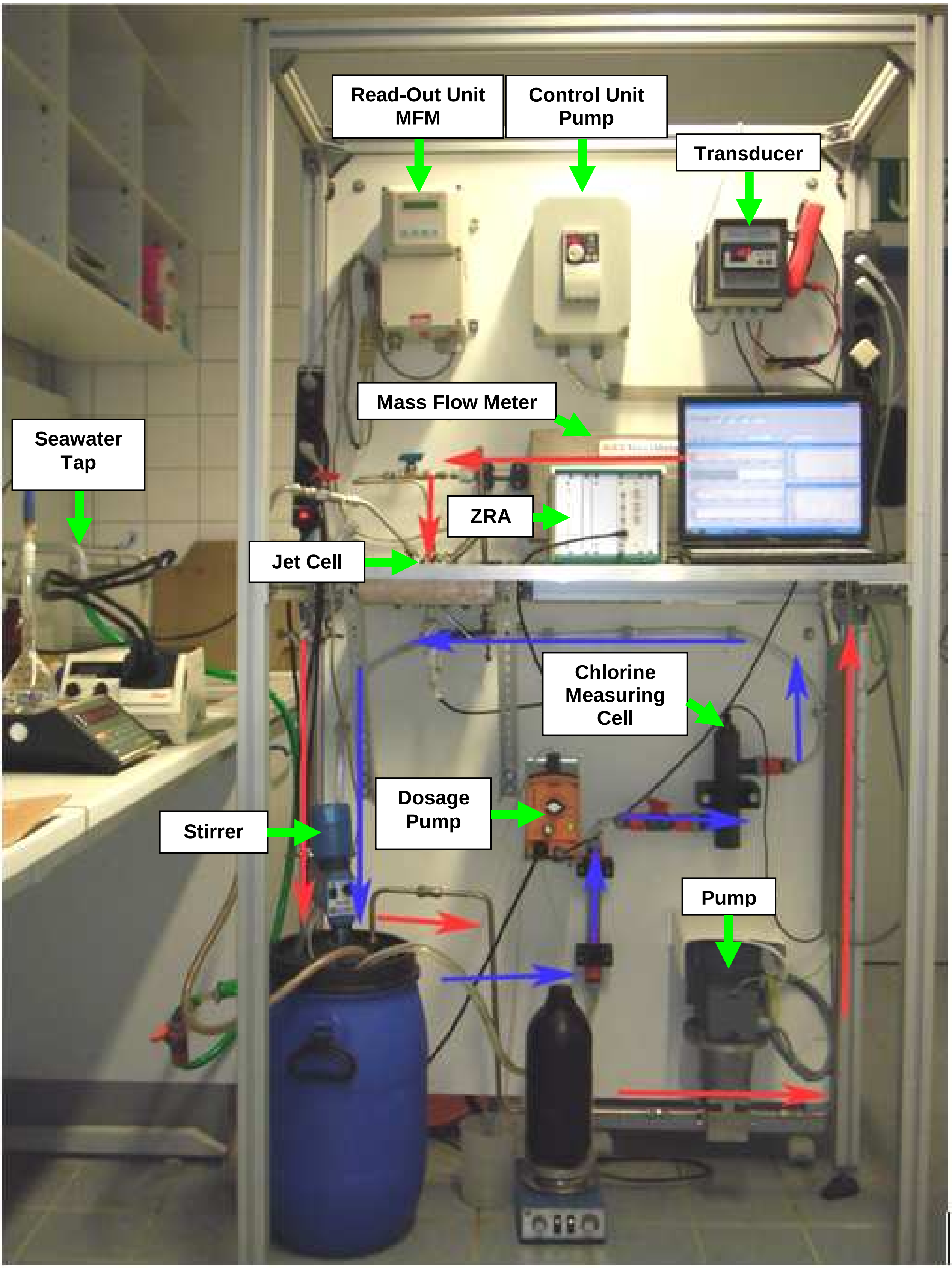

FIGURE 10 - Test rig for jet impingement experiments with natural and substitute seawater. Picture shows the set up in the Biologische Anstalt on the Isle of Helgoland, Germany.

which metered NaOCl solution into the test liquid to keep the hypochlorite concentration constant at 1 ppm (Fig. 11) over the whole test period. Indicated via a digital display the amperometric measurement yielded the concentration of "free chlorine" (including chlorine + hypochlorite) with an accuracy of 0.01 mg/L. The measuring interval was 2 minutes. The electrode was calibrated with the „CHECKIT Comperator" (Tintometer Company) using a colorimetric method. The flow at the chlorine electrode was 30 l/h. Every 10 h the buffer tank was drained and filled again with fresh Helgoland seawater which again was conditioned with hypochlorite.

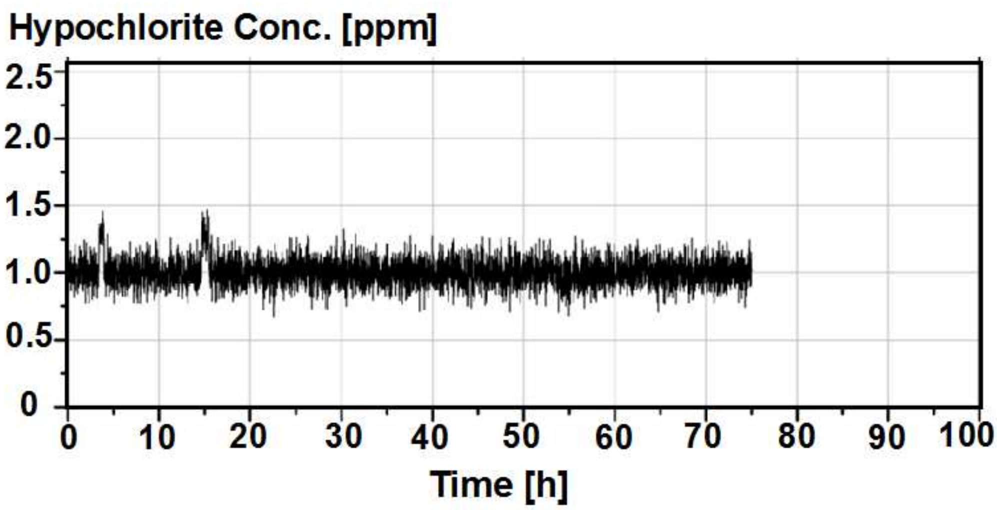

FIGURE 11 - Recording of hypochlorite concentration in the test liquid with 1 ppm hypochlorite

Experiments with substitute seawater (ASTM D1141) were performed in the same jet impingement test rig in the IFINKOR lab in Iserlohn, Germany. The test protocol was the same as with natural seawater, except that the substitute seawater was recirculated for 10 h before replenishment. Details have been described in lit. [12].

3 RESULTS

The effect of wall shear stress on the course of current noise charge vs. time curves at CuNi 90/10 and CuNi 70/30, both with as-delivered and ground surface, is plotted in Figs. 12 and 15, respectively. At a wall shear stress of 150 Pa the current noise charge curve was a straight line for a CuNi 90/10 sensor during the whole exposure time of 90 h (Fig. 12) and the noisiness of the element current was only low (Fig. 13). Increasing the wall shear stress to 160 Pa, the noise charge curve changed its slope after 21 h (Fig. 12) and at the same time the noisiness of the element current increased significantly (Fig. 14). At the end of the test period the surfaces of the sensor electrodes impinged with 160 Pa showed the start of pitting while the electrode surfaces subjected to flow with an intensity of 150 Pa exhibited a smooth uniform appearance. At higher wall shear stresses the noise charge curves changed their slope already after 8 or 12 h (180 and 170 Pa) which was accompanied by a significant increase in the noisiness of the element currents. At the end of the exposure the surfaces of the sensor electrodes appeared roughened and covered with small pits. Obviously the critical wall shear stress beyond which FILC is initiated is 150 Pa for CuNi 90/10 with ground starting surface.

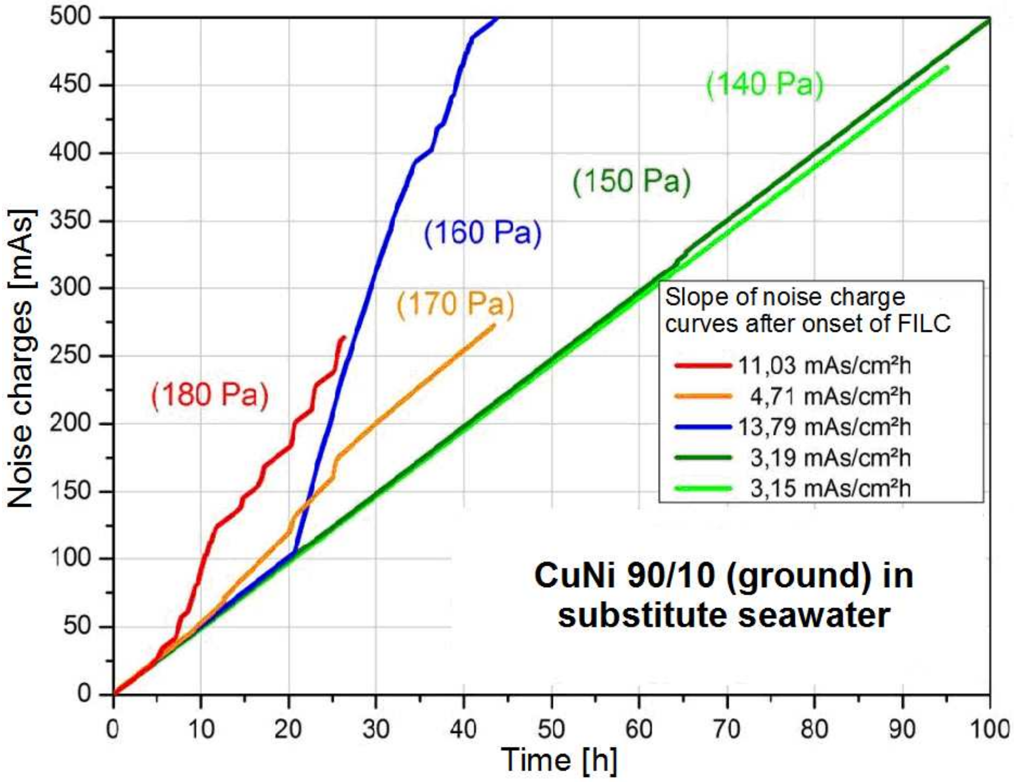

FIGURE 12 - Effect of wall shear stress on noise charge curves at CuNi 90/10 sensors with ground starting surface, impinged with substitute seawater at room temperature

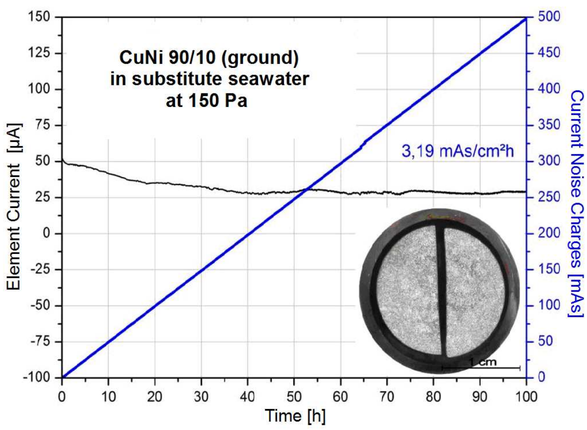

FIGURE 13 - CuNi 90/10 sensor with ground starting surface, impinged with substitute seawater at room temperature with a wall shear stress of 150 Pa

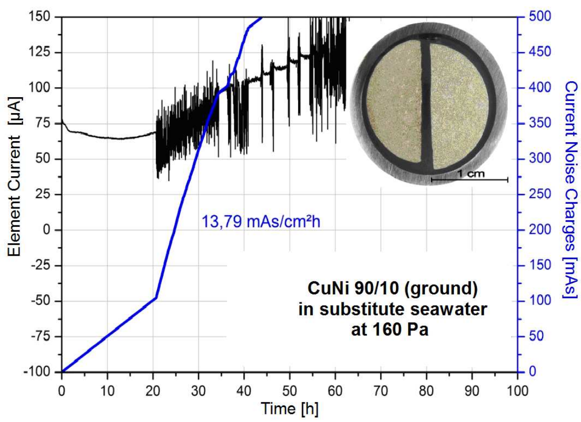

FIGURE 14 - CuNi 90/10 sensor with ground starting surface, impinged with substitute seawater at room temperature with a wall shear stress of 160 Pa

Basically the same behaviour was found for CuNi 70/30 sensors with ground starting surfaces. The difference was that the wall shear stresses beyond which FILC was initiated were higher. In this case FILC stated already at 175 Pa (Figs. 15 - 17). In all tests the onset of FILC was accompanied by an increase of the noisiness of the element currents and, consequently, by a change of the slopes of the current noise charge curves. Thus, the critical wall shear stress for CuNi 70/30 was 170 Pa for a ground starting surface.

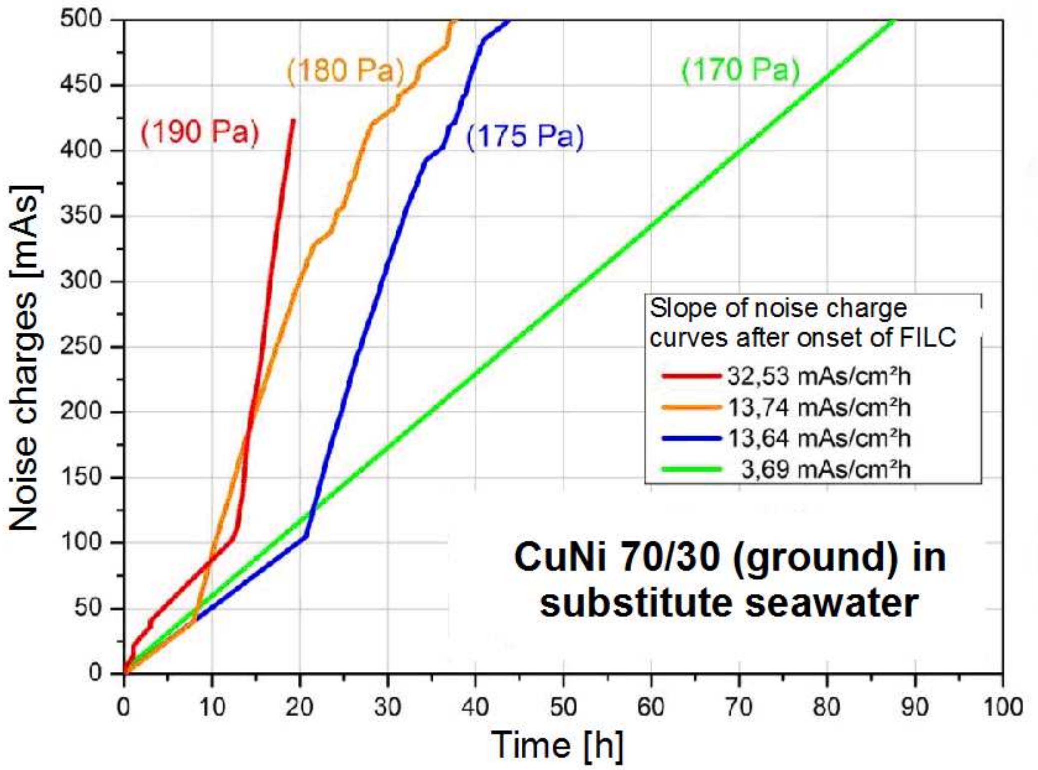

FIGURE 15 - Effect of wall shear stress on noise charge curves at CuNi 70/30 sensors with ground starting surface, impinged with substitute seawater at room temperature

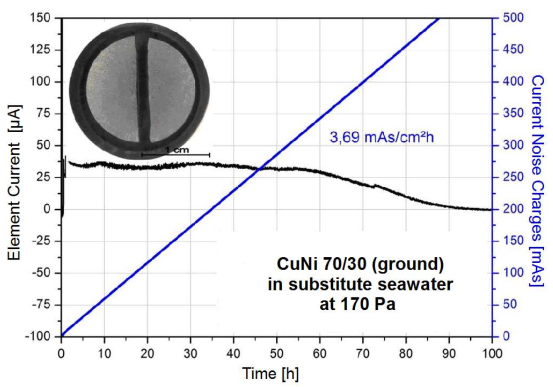

FIGURE 16 - CuNi 70/30 sensor with ground starting surface, impinged with substitute seawater at room temperature with a wall shear stress of 170 Pa

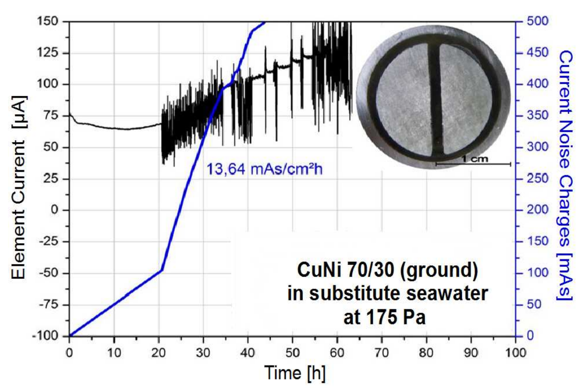

FIGURE 17 - CuNi 70/30 sensor with ground starting surface, impinged with substitute seawater at room temperature with a wall shear stress of 175 Pa

TABLE 3 - Critical Wall Shear Stresses of CuNi 90/10 and CuNi 70/30 with different surface status in different media

CuNi Alloy	Presence of Hypochlorite	Critical Wall Shear Stress [Pa]			
		Substitute Seawater (ASTM)		Natural Seawater	
		Ground Surface	6 Weeks Substitute Seawater	Ground Surface	6 Weeks Natural Seawater
CuNi 70/30	0	170	240	180	250
CuNi 90/10	0	150	220	150	220
CuNi 90/10	1 ppm	260 [a)]	>340 [a)]	110	140

[a)] from previous work [12]

It appeared that the critical wall shear stresses for the CuNi alloys tested were quite similar for untreated natural and substitute seawater, respectively. The resistance to FILC initiation was higher for CuNi 70/30 than for CuNi 90/10, although in the same order of magnitude. Conditioning (6 weeks exposure in stagnant seawater) in substitute and natural seawater, respectively, increased the resistance of both alloys to FILC significantly due to formation of protective scales. The superior performance of CuNi 70/30 appears more clearly in the pre-scaled surface mode.

Different results were obtained when the seawater was disinfected with 1 ppm hypochlorite and applied to CuNi 90/10. The critical wall shear stresses were found to be much higher in substitute seawater than in natural seawater. In natural seawater, the critical wall shear stresses were significantly lower when 1 ppm hypochlorite was present. For the pre-scaled surface mode (6 weeks exposure in stagnant natural seawater) the critical wall shear stress was even lower than under the same conditions with ground starting surfaces in hypochlorite-free natural seawater. The lowest critical wall shear stress (110 Pa) was obtained for ground starting surface in natural seawater with 1 ppm hypochlorite.

However, working with substitute seawater the critical wall shear stresses for CuNi 90/10 were found to be significantly higher in hypochlorite-containing than in hypochlorite-free substitute seawater. It must be assumed that scales formed on CuNi 90/10 in substitute seawater are improved in flow resistance by the presence of 1 ppm hypochlorite, while in natural seawater the opposite effect was observed. Presently there is no satisfactory explanation for this unexpected phenomenon.

4 CONCLUSIONS

In comparable starting surface states (ground surface or pre-scaled surface after 6 weeks exposure in substitute and natural seawater, respectively) CuNi 90/10 and CuNi 70/30 exhibit practically the same resistance to FILC in clean substitute and clean natural seawater, respectively. The critical wall shear stresses range from 150 to 180 Pa for a ground starting surface and 220 to 250 Pa for a pre-scaled surface.

The higher values apply for CuNi 70/30 which performs slightly better than CuNi 90/10.

Regardless of the type of CuNi alloy, the critical wall shear stresses range always about 70 Pa higher after pre-scaling than with ground starting surface.

The presence of 1 ppm hypochlorite reduces the FILC resistance of CuNi 90/10 in case of natural seawater (critical wall shear stresses from 150 to 110 Pa for ground surface and from 220 to 140 Pa for pre-scaled surface), but, surprisingly, increases the FILC resistance in case of substitute seawater (critical wall shear stresses from 150 to 260 Pa with ground surface and from 220 to >340 Pa with pre-scaled surface).

Even under unfavourable environmental conditions (e.g. 1 ppm hypochlorite in natural seawater) the critical wall shear stresses, evaluated in this study for CuNi 90/10 and CuNi 70/30 are significantly higher than the critical wall shear stresses reported in the literature (Table 1). It is concluded that these literature values are much too conservative and that the FILC resistance of these CuNi alloys is significantly higher.

5 ACKNOWLEDGEMENTS

The authors thank the Biologische Anstalt Helgoland of the Alfred Wegener Institute for Polar and Marine Research, specifically Prof. Dr. Karen Helen Wiltshire, for the opportunity to run jet impingement experiments in their labs with Helgoland seawater and KME Germany AG for financial support and the permission to publish this paper.

6 REFERENCES

1. G. Schmitt, M. Bakalli, "Flow Assisted Corrosion", in "Schreir's Corrosion", Vol. 2 2010) pp. 954-987, J.. Richardson et al. (eds.), Shreir's Corrosion. Amsterdam: Elsevier; Fourth Edition 2010.
2. G. Schmitt, M. Bakalli
"A Critical Review on Measuring Techniques for Corrosion Rates under Flow Conditions", Power Plant Chemistry, **9** (2007) 89.
3. G. Schmitt, M. Bakalli, "Advanced Models for Erosion Corrosion and its Mitigation", Materials and Corrosion 59 (2008)(2)181-192.
4. G. Schmitt, M. Bakalli, "Initiation of Flow Induced Localized Corrosion - Correlation between Wall Shear Stresses and Freak Energy Densities", Proc. 9th Symp. Electrochem. Methods in Corrosion Research (9EMCR), June 18-23, 2006, Dourdan/France.
5. R.H. Hausler, G. Schmitt, „Hydrodynamic Flow Effects on Corrosion Inhibition“ CORROSION‘2004, NACE International, Houston/Texas, Paper 04-402.
6. C. A. Powell, H. T. Michels, „Copper-Nickel Alloys for Seawater Corrosion Resistance and Antifouling - A State of the Art Review“, CORROSION 2000, NACE International, Houston, Texas, USA, 2000, Paper 627.
7. C. A. Powell, „Copper Nickel Alloys - Resistance to Corrosion and Biofouling, CDA Inc. Seminar Technical Report 7044 - 1919, The Application of Copper Nickel Alloys in Marine Systems“, 1992, http://www.copper.org, extracted 25.04.2009.
8. F. P. Ijsseling, „The Corrosion Behaviour of the System CuNi10Fe/Seawater. The Protective Layer of Corrosion Products - A Literature Review", Reviews on Coatings and Corrosion: A Quarterly Reviews, **3** (1981) 269 – 324.
9. K,D. Efird, Effect of Fluid Dynamics on the Corrosion of Copper-Base Alloys in Sea Water", Corrosion 33 (1973)(1) 3-8.
10. A.H. Tuthill, "Guidelines for the Use of Copper Alloys in Seawater", Materials Performance 26 (1987)(9) 12-22.
11. W. Schleich, R. Feser, G. Schmitt, K. Schnier, T. Gommlich, S. Günther,
"Corrosion Behaviour of Copper-Nickel Alloy CuNi90/10 in Chlorinated Seawater", Proc. EUROCORR‘2007, Sept.09-13, 2007, Freiburg, Germany260.
12. W. Schleich, R. Feser, G. Schmitt, K. Schnier, T. Gommlich, S. Günther
„Effect of Seawater Chlorination on the Corrosion Behaviour of Copper-Nickel Alloy CuNi90/10", CORROSION'2008, NACE International, Houston/Texas, 2008, Paper 08-231.
13. F. Giralt, O. Trass, Canadian J. Chem. Eng. **53** (1975) 505-511.
14. F. Giralt, O. Trass, Canadian J. Chem. Eng. **54** (1976) 148-155.
15. G. Schmitt, R.Buschmann, K.-F. Foehn, H. Theunissen, "Bimetallic ECN Sensor for Monitoring Inhibitor Efficiency in Water-based Hydraulic Fluids", CORROSION'2005, NACE International, Houston/Texas, 2005, Paper 05-382
16. G. Schmitt, R. Buschmann, Ch. Olry, B. Motko, P. Schrems,
„Measuring Corrosivity as Simple as Temperature?
CORROSION'2007, NACE International, Houston/Texas, 2007, Paper 07-379.